

Research Article pubs.acs.org/acscatalysis

Effect of Water on Cumene Dealkylation over H-ZSM-5 Zeolites

Han K. Chau, Hien D. Mai, Abhishek Gumidyala, Tram N. Pham, Dai-Phat Bui, Andrew D. D'Amico, Ismaeel Alalq, Daniel T. Glatzhofer, Jeffery L. White, and Steven P. Crossley*



Cite This: ACS Catal. 2023, 13, 9158-9170



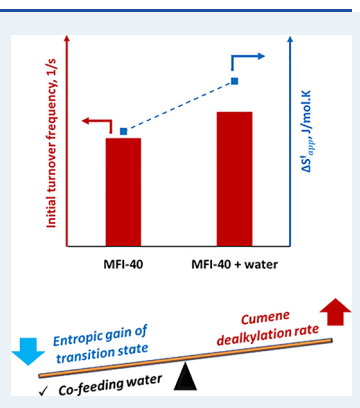
ACCESS I

III Metrics & More

Article Recommendations

Supporting Information

ABSTRACT: The influence of water on Brønsted acid chemistry has been studied extensively recently for the conversion of oxygen-containing reactants. The effect of water on hydrocarbon transformations is far less explored and understood. Here, we show that cumene dealkylation over H-ZSM-5 zeolites is strongly influenced by the location of Brønsted acid sites and the presence of water molecules inside zeolite pores. While increasing acid site density leads to enthalpic stabilization of both adsorbed states and transition states due to a greater fraction of acid sites within more confined voids, the presence of water enhances rates via entropic stabilization of transition states at the expense of an increased intrinsic activation enthalpy. Both effects of water and the acid site location on the improving reaction rate are discussed. This direct participation of water is contrasted with water-induced modifications to the catalyst surface, such as the generation and mobility of extra-lattice species. These extra-lattice species have been shown to influence reaction rates for more demanding chemical transformations such as alkane cracking but are less effective at promoting the facile dealkylation chemistry studied here. We further reveal how the addition of moisture also induces positive consequences on catalyst stability by limiting subsequent oligomerization reactions with formed products.



KEYWORDS: zeolites, dealkylation, water effect, site proximity, deactivation

1. INTRODUCTION

Collective understanding of the role of water in acid-catalyzed chemistry is continuously evolving. Water has been traditionally considered a simple diluent for gas phase cracking chemistry, but it may not be a simple benign spectator. Local perturbations to the zeolite structure induced by water can significantly alter the environment around protons through the creation of extra-lattice species and consequentially significantly modify activity for demanding transformations such as alkane cracking. It has also been reported that water may directly influence rates of certain reactions, such as alcohol dehydration, by creating more stable hydrogen-bound surface intermediate species. Interactions of water that modify reaction rates of more facile reactions with hydrocarbons, such as dealkylation of aromatics, have not been explored to the same extent. Practical considerations, however, necessitate a more detailed understanding of the impact that water has on this type of chemistry. Dealkylation of aromatics has a profound impact on benzene yield in fluidized catalytic cracking, as well as emerging applications such as the catalytic conversion of polystyrene to value-added products.

Dealkylation of alkylbenzenes over zeolites has been studied for many years as this is a critical reaction involved in the production of a variety of high-value chemicals.³⁻⁶ In fact, cumene dealkylation has been used as a test reaction to characterize catalyst acidity and study the mechanism of industrial catalytic cracking since the early 1950s. While both reaction products, benzene and propylene, are high-value

commodity chemicals, the formation of benzene is of great interest to crude oil refineries due to benzene concentration limits in gasoline. However, there have been only a few attempts to elucidate the mechanism of cumene dealkylation over zeolites. 7,8 The influence of water on cumene dealkylation has not been investigated in the literature, although steam is normally used to transport vaporized feed streams with a powdered catalyst up a riser and strip hydrocarbon products from catalyst particles in fluid catalytic cracking processes.

Zeolites are among the most industrially important solid acid catalysts that have been used in various chemical transformations for several decades. The presence of aluminum in a zeolite framework creates a negative charge that is neutralized by cations such as protons or metals. Recently, the distribution of aluminum in terms of crystallographic unique T-site location and proximity between aluminum species has attracted much attention. 10 In fact, the proximity of Brønsted acid sites influences reaction rates of alkane cracking and olefin oligomerization and reaction pathways of aldol condensation and alcohol dehydration. ^{2,11–16} Vicinal Brønsted acid sites

Received: November 23, 2022 Revised: June 13, 2023 Published: June 26, 2023





have been reported to modify the turnover frequency of some hydrocarbon transformations by increasing activation entropy, 11,13,14 while modified stability of the active intermediate and a shift in the reaction pathways have been reported for the presence of paired sites in the case of alcohol dehydration.² In terms of acid strength, it was reported by Iglesia and coworkers that the strength of the Brønsted acid site in zeolites does not significantly depend on acid site density in MFI framework zeolites, framework structures, or proton locations. 17,18 Instead, rates were reported to correlate to the greatest extent with the local confining environment around the transition state. Unraveling these effects is quite challenging, as lowering the Si/Al ratio of a zeolite in its protonated form increases the Brønsted acid site density. This often leads to both an increase in the concentration of paired sites, as well as modifications to the location of acid sites. The confining local environment around a Brønsted acid site has been shown to influence the catalytic activity of zeolite catalysts in many reactions such as alkane cracking and alcohol dehydration. $^{19-21}$ The presence of extra-framework aluminum species is another important factor that could alter the local environment around an acid site while also influencing reaction transition states, leading to the changes in catalytic activity by entropic or enthalpic stabilization.²²

The effect of water on the zeolite structure and catalytic reactivity has been studied extensively for both liquid and vapor phase reactions.^{27–32} In terms of zeolite structure stability, the hydrolysis of Si-O-Si and Si-O(H)-Al, as well as amorphization at silanol defects, can occur depending on the phase of water and reaction temperature, leading to a loss of crystallinity and catalyst destruction. The presence of water molecules inside zeolite pores can influence reactivity by changing mass transfer properties of reactants and products, enthalpic stabilization of reactants or transition states through solvation, facilitating proton transfer, and remote bond polarization. 15,27,33 On the other hand, it is known that water molecules can interact with the acidic zeolites, facilitate proton delocalization at Brønsted acid sites, and form hydronium ion clusters around the framework site. 34-37 The presence of a delocalized proton in a hydronium ion cluster created by the presence of water near a conventional Brønsted acid site in zeolites is capable of catalyzing aqueous phase reactions such as cyclohexanol dehydration and alkylation of phenolic compounds with alcohols.^{38–41} Hydronium ions have been proposed to generate a highly local ionic environment that can modify transition states for some reactions, but this effect becomes less pronounced at high concentrations of hydronium ion clusters due to spatial constraints. 42 The role of water on zeolite catalyst stability is intriguing. While enhancing catalyst lifetime by co-feeding water has been generally attributed to competitive adsorption of water molecules, 43,44 it was reported for methanol-to-hydrocarbon reactions that water could reduce catalyst deactivation by shifting the equilibrium constants of surface intermediates, effectively decreasing the rate of initiation and termination reactions that ultimately lead to catalyst deactivation.45

Here, we report the enhancement of reaction rates and changes in catalyst stability during cumene dealkylation over H-ZSM-5 zeolites in the presence of varying density, proximity, and location of acid sites and the inclusion of co-fed water, with reversible rate modifications that contrast the role that water commonly plays on more demanding alkane cracking reported in previous studies.²⁵ This motivated us to system-

atically study the effect of water over MFI samples with varying Si/Al ratios on the intrinsic kinetic constants associated with cumene dealkylation over H-ZSM-5 zeolites. Different H-ZSM-5 zeolites with varying fractions of paired acid sites and site locations were used as catalysts for cumene dealkylation in the absence and presence of co-fed water. Extra-framework aluminum species were removed to decouple the roles of water and acid site proximity from the presence of extra-lattice species on catalytic activity and catalyst deactivation during cumene dealkylation over H-ZSM-5 zeolites.

2. EXPERIMENTAL SECTION

2.1. Catalyst Preparation. ZSM-5 zeolites with different Si/Al ratios (CBV-2314 with Si/Al = 11.5, CBV-3024E with Si/Al = 15, CBV-8014 with Si/Al = 40, CBV-28014 with Si/Al = 140) were purchased in ammonium forms from Zeolyst International. In order to decouple the role of extra-framework aluminum species (EFAL) from site proximity, the ZSM-5 catalyst with a Si/Al = 11.5 was treated by (NH₄)₂SiF₆ (AHFS, Sigma-Aldrich, 99.999%, trace metals basis) solution. A mixture of 2.06 g of NH₄-ZSM-5 and 1.92 g of AHFS was added to 80 mL of water. The amount of AHFS was about four times the amount of aluminum in NH₄-ZSM-5 (Si/Al = 11.5). The mixture was stirred vigorously at 80 °C for 5 h. The mixture was centrifuged, and the solid part was washed five times with hot deionized water, followed by a drying step at 80 °C in a vacuum oven for 15 h.

All catalyst samples were calcined in flowing dry air with a ramping rate of 2 °C/min up to 600 °C and kept at that temperature for 5 h to obtain proton-form H-ZSM-5. Protonated zeolites were then pelletized, crushed, and sieved to particles with sizes ranging from 90 to 250 μ m. H-ZSM-5 zeolites with Si/Al = 11.5, Si/Al = 40, and Si/Al = 140 are denoted as MFI-11.5, MFI-40, and MFI-140, respectively. The catalyst sample after AHFS treatment is denoted as AHFS-MFI-11.5.

2.2. Catalyst Characterization. Temperature-programmed reaction of isopropylamine (IPA-TPRx) in combination with an MKS Cirrus 200 quadrupole mass spectrometer (MS) was carried out on catalyst samples to determine Brønsted acid site (BAS) densities of these catalysts. The details of this method are described elsewhere. 46

Fourier-transform infrared (FT-IR) spectroscopy was carried out using a PerkinElmer Spectrum 100 Fourier Transform Infrared (FT-IR) spectrometer equipped with a high-temperature diffuse reflectance Infrared Fourier Transformation (DRIFT) CaF $_2$ cell (HVC, Harrick). A blank run using a KBr pellet was obtained for the background. Catalyst samples were ground and pressed into a sample holder equipped with a thermocouple. The sample was pretreated at 300 $^{\circ}\text{C}$ for 1 h using He as a carrier gas to remove physically adsorbed water in the catalyst. FT-IR spectra of MFI-11.5 and AHFS-MFI-11.5 were obtained at 300 $^{\circ}\text{C}$.

¹H MAS NMR spectra were acquired by placing reactants and zeolites inside an enclosed zirconia rotor followed by a temperature ramp. Spectra were acquired with a 90° pulse, a recycle delay of 2 s, and 4 kHz MAS spinning. SEM images were collected on a Zeiss Neon with an in-lens backscatter detector.

The heat of adsorption data were collected using a Micromeritics ASAP 2020 (with micropore, vapor, and hydrocarbon options) coupled with a Sertaram C80 Calvet calorimeter. Approximately 100 mg of each sample was heated

under vacuum to 325 °C at 5 °C/min and held for 10 h on the ASAP 2020 degas ports. The sample was then transferred to the C80 and heated at 5 °C/min to the analysis temperature— 100 °C. The heat flow signal was stabilized at the analysis temperature for approximately 3 h. Custom cells built in-house were used on the calorimeter. An empty cell, identical in construction to the sample cell, was placed in the reference chamber of the calorimeter. The analysis temperature of 100 °C was chosen in order to be low enough to avoid reaction of the cumene with the sample but high enough to avoid weak physisorption. Each dose of cumene was approximately 6.5 μ mol (or 65 μ mol/g).

The density of Al in pairs in ZSM-5 zeolites was quantified using cobalt exchange. Specifically, the proton form (1.0 g) of fresh ZSM-5 zeolites with different Si/Al ratios (i.e., MFI-140, MFI-40, MFI-15, MFI-11.5, and AHFS-MFI-11.5) were treated with 90 mL of 0.10–0.25 M Co(NO₃)₂ solution for 24–72 h at 70 °C. Afterward, the solid catalysts were centrifuged and washed five times with DI water, followed by drying overnight at 80 °C and calcinating at 550 °C for 5 h. The BAS densities of the cobalt-exchanged zeolites were measured by IPA-TPRx.

2.3. Catalytic Testing. Vapor phase flow reactions at atmospheric pressure over H-ZSM-5 catalysts were conducted in a quartz tube reactor (1/4" OD). The catalyst was mixed with acid-washed glass beads and packed between quartz wool layers in the quartz reactor. The quartz reactor was installed inside a temperature-controlled oven. The temperature of the catalyst bed was controlled by a thermocouple located inside the quartz reactor beneath the catalyst bed. Catalyst samples were pretreated at 300 °C for 1 h with helium as a carrier gas (125 mL/min) to remove physisorbed water in the catalyst. After pretreatment, the temperature of the oven was set to reach the reaction temperature. Cumene (Sigma Aldrich, 98%) and de-ionized water were fed through inlet septa into the reactor using KD Scientific syringe pumps. The inlet of the reactor was heated to create a vaporization zone for the liquid reactants. The outlet of the reactor was heated to 250 °C to prevent condensation of products on the downstream tubing. Samples were collected at different reaction time on stream (TOS) using a gas sample loop connected with a six-port valve and products were analyzed using a Hewlett Packard 6890 gas chromatograph equipped with a flame ionization detector and an INNOWAX column (30 m \times 0.25 mm).

A micro-pulse reactor was used to measure the catalytic activity for cumene dealkylation to minimize the influence of catalyst deactivation. Pelletized H-ZSM-5 (5-15 mg) mixed with 95 mg glass beads was utilized for the reaction. After the catalyst was pretreated at 300 °C for 1 h, several pulses of 0.15 μ mol cumene, diluted in N₂, were sent over the catalyst bed at a 75 mL/min N₂ flowrate. The volume of the sample loop was 500 μ mol and the partial pressure of cumene in the loop was 1.17 kPa. After conversion was measured for cumene dealkylation on the parent zeolite, pulsed water was utilized to treat the catalyst under conditions that lead to a significant enhancement for the rates of alkane cracking reactions. 25 The catalyst was exposed to 20 pulses of vapor water at 480 °C and then dried overnight. Each pulse contains 2.85 µmol of water at a partial pressure of 18.6 kPa. The detailed conditions for this treatment are listed elsewhere.²⁵ The temperature of the pulse reactor was then reduced to a reaction temperature of 300 °C to measure the reactivity for cumene dealkylation. Products of the reaction were analyzed by GC-FID.

To decouple kinetic effects from catalyst deactivation over the reaction time on stream in flow reactions, all of the reaction rates were extrapolated to zero-time on stream to obtain initial rates. Turnover frequency (TOF) and turnover number (TON) for a reaction are defined as follows:

Furnover frequency $= \frac{\text{Reaction rate (mol of cumene converted per second per gram catalyst)}}{\text{Brønsted acid site density (mol H}^{\dagger}\text{per gram catalyst)}} (1/s)$ (1)

Turnover number =
$$\int_{0}^{t} TOF(t) dt$$
 (2)

where TOF(t) is the turnover frequency at the reaction time on stream t.

3. RESULTS AND DISCUSSION

3.1. Cumene Dealkylation over H-ZSM-5 Zeolites in the Absence of Water. Cumene dealkylation has been proposed to occur on Brønsted acid sites through cleavage of the C–C bond of a protonated cumene molecule to form benzene and a propyl carbocation that can desorb to form propylene. Therefore, the products of cumene dealkylation are benzene and propylene with an expected stoichiometric 1:1 molar ratio.

Catalytic activities of H-ZSM-5 zeolites with different features such as Brønsted acid site density, fraction of paired sites and extra-framework aluminum species, and location of acid sites were investigated for cumene dealkylation. Brønsted acid site densities of H-ZSM-5 zeolites in this study are shown in Table S1. FT-IR spectra in Figure S1 show a peak corresponding to extra-framework aluminum species in MFI-11.5 at a wavenumber of 3643 cm $^{-1}$, located between typical bands for surface silanol (\equiv Si-(O-H)) at 3737 cm $^{-1}$ and surface Brønsted acid sites (\equiv Si-(O-H)-Al \equiv) at 3596–3599 cm $^{-1}$, while the peak of extra-framework aluminum species is not present in AHFS-MFI-11.5. These results indicate that extra-framework aluminum species have been removed successfully by AHFS treatment, while the vast majority of the Brønsted acid sites were preserved.

As shown in Figure 1, the initial rate normalized per proton, or turnover frequency (TOF), on different H-ZSM-5 zeolites for cumene dealkylation exhibits the following order: MFI-11.5 > AHFS-MFI-11.5 > MFI-40 > MFI-140. The reactivity appears to strongly depend on the location and distribution of Brønsted acid sites. It has been previously reported that

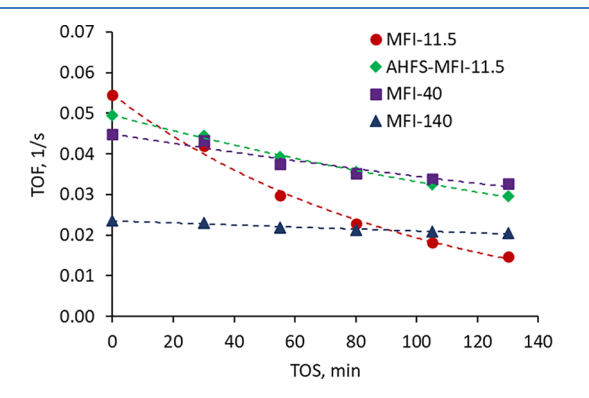


Figure 1. Rate of cumene dealkylation over different zeolites at a reaction temperature of 300 $^{\circ}$ C as a function of time on stream (TOS), $P_{\text{cumene}} = 0.5 \text{ kPa}$.

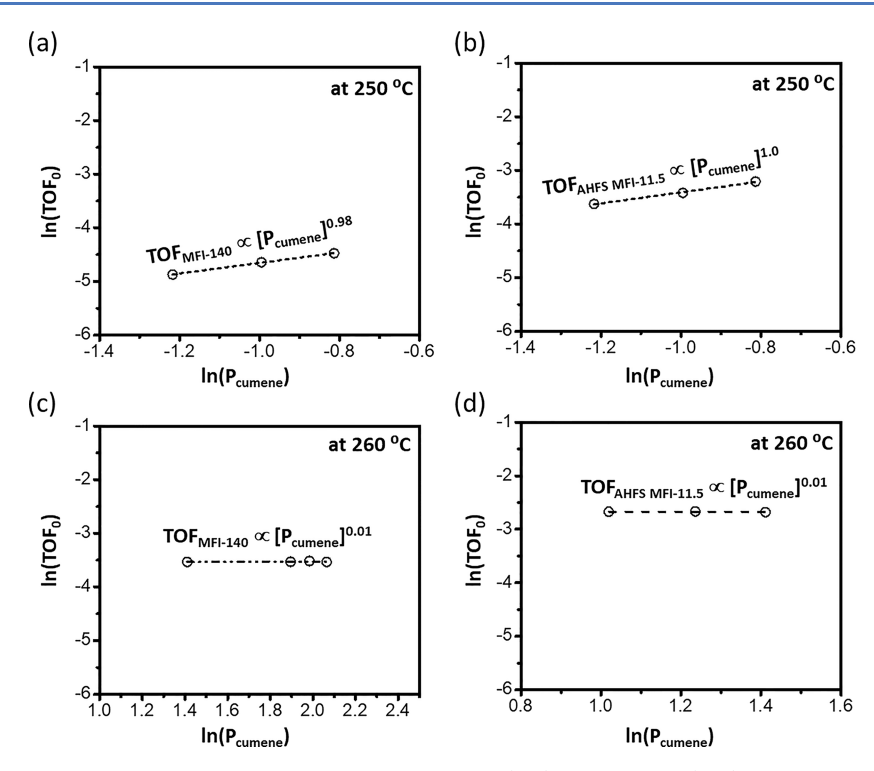


Figure 2. Cumene dealkylation reaction in the first and zero-order regimes over (a, c) MFI-140 and (b, d) AHFS-MFI-11.5 in the absence of water ($P_{\text{water}} = 0 \text{ kPa}$) at 250 and 260 °C. The conversion for MFI-140 and AHFS-MFI-11.5 was kept below 12 and 16%, respectively.

Brønsted acid sites are favorably located at large pore intersection voids in low Brønsted acid site density zeolites such as MFI-140 and MFI-40.¹⁷ Based on this, one could assume that Brønsted acid sites are located in more confined straight channels and sinusoidal channels in zeolites with lower Si/Al ratios such as MFI-11.5 and AHFS-MFI-11.5 catalysts. In addition, the amount of extra-framework aluminum species in MFI-40 and MFI-140 is negligible because the measured framework Brønsted acid site densities by IPA-TPRx are very close to the theoretical values. Therefore, any differences in the reaction rate over MFI-40 compared to MFI-140 could be attributed to the proximity of Brønsted acid sites on cumene dealkylation chemistry.

Wichterlová and co-workers reported that the distribution of proximate framework Brønsted acid sites in ZSM-5 zeolites can be probed by Co²⁺ ion exchange.⁴⁷ This method was applied by other research groups illustrating the correlation between proximate framework Brønsted acid sites, or paired sites, and Si/Al ratios. 11,48,49 The fraction of paired sites decreases with an increase of the Si/Al ratio or a lowering of the Brønsted acid site density of H-ZSM-5 zeolites, as shown in Table S2 and Figure S2. Contrasting rates observed in Figure 1 with the fraction of paired sites as shown in Figure S3, one notes that there is a significant difference between the catalyst with the highest population of paired sites (MFI 11.5) and the catalyst with the lowest population of paired sites (MFI 140). This behavior could be explained by the concentration of paired sites as well as the local environment surrounding the active site, which will be discussed in more detail in the next section.

There is an insignificant number of paired sites in the MFI-140 catalyst (0.01 mmol/g). On the other hand, a significant number of Brønsted acid sites in MFI-40 (0.12 mmol/g) and particularly in MFI-11.5 (0.68 mmol/g) are paired, or in close proximity, based on Co^{2+} exchange (Table S2). In addition, there is only a small loss of the Brønsted acid site density in

AHFS-MFI-11.5 (10%) after acid treatment when compared to the parent zeolite MFI-11.5. Therefore, it is expected that the number of paired sites in AHFS-MFI-11.5 is smaller than that in MFI-11.5, but still quite significant. Also, we found that the tested zeolites, namely, MFI-140, MFI-40, and AHFS-MFI-11.5, can reach zero-order regime (Figures 2 and S4), revealing that mass transport is not a limiting factor in the cumene dealkylation reaction over these studied catalysts. Further discussions are given in the following sections.

3.2. Decoupling Contributions in Rate Due to Confinement and Proximate Sites. We speculate that both proximity of acid sites and the local confining environment surrounding active sites can influence cumene dealkylation rates. By comparing rates as a function of temperature for these catalysts after carrying out the reaction in the first-order regime from 250 to 300 °C, we identify the apparent activation enthalpy and entropy over these three different catalysts. Conversion levels and product distributions can be found in Figure S5. Table 1 reveals that while there is a significant enhancement in reaction rates observed when contrasting MFI-11.5 from the other samples (Figure 1), the MFI-40 and MFI-140 samples exhibit statistically indistinguishable activation energies. This result suggests that the

Table 1. Apparent Activation Energies Measured in the Absence of Water

catalysts	apparent activation energy $E_{\rm app}~({\rm kJ/mol})^a$
AHFS-MFI-11.5	21.2 ± 1.4
MFI-40	39.7 ± 2.7
MFI-140	36.5 ± 1.6

"Obtained from Arrhenius plot under first-order reaction conditions with respect to cumene in the temperature range of 250–300 °C. The standard errors are estimated from the least squares method.

paired sites, which are present in much higher quantity in the MFI-40 sample when contrasted with the MFI-140 sample, are not the primary contributing factor to activation energy reductions. We note that, while the differences in rate when proximate sites are varied in this case are modest, significant differences have been observed in other studies. For example, upon studying propylene oligomerization and alkane cracking over ZSM-5 and CHA zeolites, similar apparent activation enthalpy but less negative apparent activation entropy values were reported on proximate sites compared to those observed on isolated sites. 11,13,14 We reiterate that the opposite trend is observed in this case where the apparent activation enthalpy for AHFS-MFI-11.5 with the presence of paired sites and an insignificant amount of extra-framework aluminum species is lower than those for MFI-40 and MFI-140 (Table S3). Rather, these results suggest that the predominant factor that influences the apparent barrier is the confinement around the active site. The confinement effect present in the sample with higher site density has been observed for reactions such as cracking⁵⁰ and etherification¹⁷ as the Al content in MFI samples increases.

While these results strongly suggest that the primary contribution is the more confining environment surrounding the active site, as opposed to paired sites, they do not reveal if these differences are due to the stabilization of transition states or reactive intermediates. In order to assess this further, we have carried out experiments at varying partial pressures of cumene and adjusted temperatures to achieve low conversion levels (Figure S6). This is essential to obtain more precise rates while minimizing contributions of reaction products on measured rate constants in order to decouple entropic and enthalpic contributions to reaction rates. Because the MFI 11.5 and MFI 140 exhibit the greatest difference in reactivity, we focus primarily on these two samples hereafter.

Figure 2 reveals that we have been able to achieve reaction conditions between the temperature range of 250–260 °C, where the reaction operates fully in the 1st and 0th order regime. Because enthalpies of adsorption are negative, the coverage of reactants will decline as temperature increases. Identifying temperatures where the reaction proceeds as 1st order at the lowest temperature studied guarantees that it remains in the 1st order regime as the temperature is increased. Similarly, by identifying pressures where the surface is saturated with cumene at the highest temperature used for barrier measurements, the same argument above persists and the true intrinsic barrier will be measured across the temperature range studied.

Barriers measured under these temperature ranges agree quite well with those measured above during the first-order regime at higher temperatures, with indistinguishable activation energies measured across the temperature ranges (Table 2).

Contrasting the 0th order and 1st order regimes for cumene dealkylation over these two samples reveals several important findings. First, the intrinsic barriers measured under conditions where the surface is saturated by cumene reveal that the intrinsic activation energy is indeed lower over the AHFS-MFI-11.5 sample when contrasted with the MFI-140 sample (Table 2, Figures S7 and S8), indicating that the confining environment of the former does not only stabilize reactive intermediates, but preferentially stabilizes the kinetically relevant transition state. Furthermore, the negative intrinsic activation entropy observed in the 0th order regime over both

Table 2. Intrinsic and Apparent Activation Energies, Enthalpies, and Entropies Measured in the Absence of Water in the Temperature Range of 250–260 °C

	catalysts	AHFS-MFI-11.5	MFI-140
zero-order regime	intrinsic activation energy $E_{\text{int}} (kJ/\text{mol})^a$	112.1 ± 5.3	120.5 ± 2.8
	intrinsic activation enthalpy $\Delta H_{\mathrm{int}} \left(\mathrm{kJ/mol}\right)^b$	107.7 ± 5.3	116.2 ± 2.8
	intrinsic activation entropy $\Delta S_{\text{int}} (J/\text{mol-K})^b$	-69.9 ± 10.0	-61.2 ± 5.3
first-order regime	apparent activation energy $E_{\text{app}} (kJ/\text{mol})^a$	19.7 ± 1.1	37.5 ± 0.9
	apparent activation enthalpy $\Delta H_{\mathrm{app}}^{\ddagger}\left(\mathrm{kJ/mol}\right)^{b}$	15.3 ± 1.1	33.1 ± 0.9
	apparent activation entropy $\Delta S_{\text{app}}^{\ddagger} \left(\text{J/mol·K} \right)^b$	-248.7 ± 2.1	-224.7 ± 1.7

"Obtained from Arrhenius plot conditions in the temperature range from 250 to 260 °C. ^bCalculated from the transition state theory using the temperature range from 250 to 260 °C. The standard errors are estimated from the least squares method.

catalysts reveals that the reaction proceeds through an early transition state, as this reaction creates two products that will ultimately result in substantial entropic gains. An early transition state indicates that the transition state exhibits fewer degrees of freedom than the adsorbed reactant intermediate, which can only be possible if the said transition state arrives early along the reaction path.

In addition to increased stabilization of the transition state in reference to the adsorbed state discussed above, the more confined environment surrounding the active sites in the AHFS-MFI-11.5 sample also preferentially stabilizes reactive intermediates. This is revealed by a greater difference in activation enthalpy observed in the 0th order vs 1st order regime for the AHFS-MFI-11.5 sample when compared with the MFI-140 sample, revealing a greater adsorption enthalpy in the former sample by approximately 10 kJ/mol. This trend agrees quite well with experimental adsorption enthalpies measured independently through calorimetric measurements of these two samples, where the heat of adsorption of cumene estimated by calorimetry on high Si/Al MFI zeolite MFI-140 was 90 kJ/mol, increasing to 101 kJ/mol over AHFS MFI-11.5.

3.3. Discerning the Role of Extra-Framework Al Species and Synergistic Sites. As noted above, the high site density samples were acid-washed to remove extra framework Al species that have been shown to contribute to rates of certain reactions to avoid complicating the analysis. In order to investigate the role of these species further, role of extra-framework aluminum species in association with water in the low Si/Al zeolite MFI-11.5 was further clarified by the pulsed water experiment (Figure 3). As reported previously, the pulsed water treatment does not create a persistent water partial pressure nor does it lead to the loss of Brønsted acid sites or significant modifications in the crystallinity of H-ZSM-5 catalysts. 25 However, we have shown that this treatment can facilitate the mobility of extra-framework aluminum species that are already present, leading to the formation of synergistic sites between Brønsted acid sites and neighboring extraframework aluminum species. These synergistic sites are important for alkane cracking reactions, which happen at higher temperatures than cumene dealkylation and usually require high activation energy to protonate alkane molecules.

The pulsed water treatment was conducted under the same conditions that significantly enhanced the reactivity of zeolites

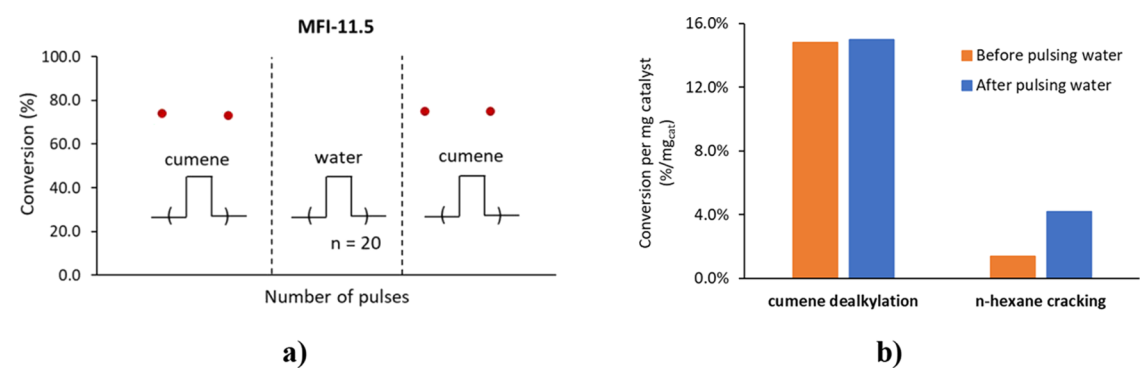


Figure 3. (a) Conversion of cumene before and after pulsing water over 5 mg of MFI-11.5 at a reaction temperature of 300 °C; (b) compare conversion of cumene dealkylation (T = 300 °C, $P_{\text{cumene}} = 1.17$ kPa) and n-hexane cracking (T = 480 °C, $P_{n\text{-hexane}} = 4.5$ kPa)²⁵ before and after pulsing water.

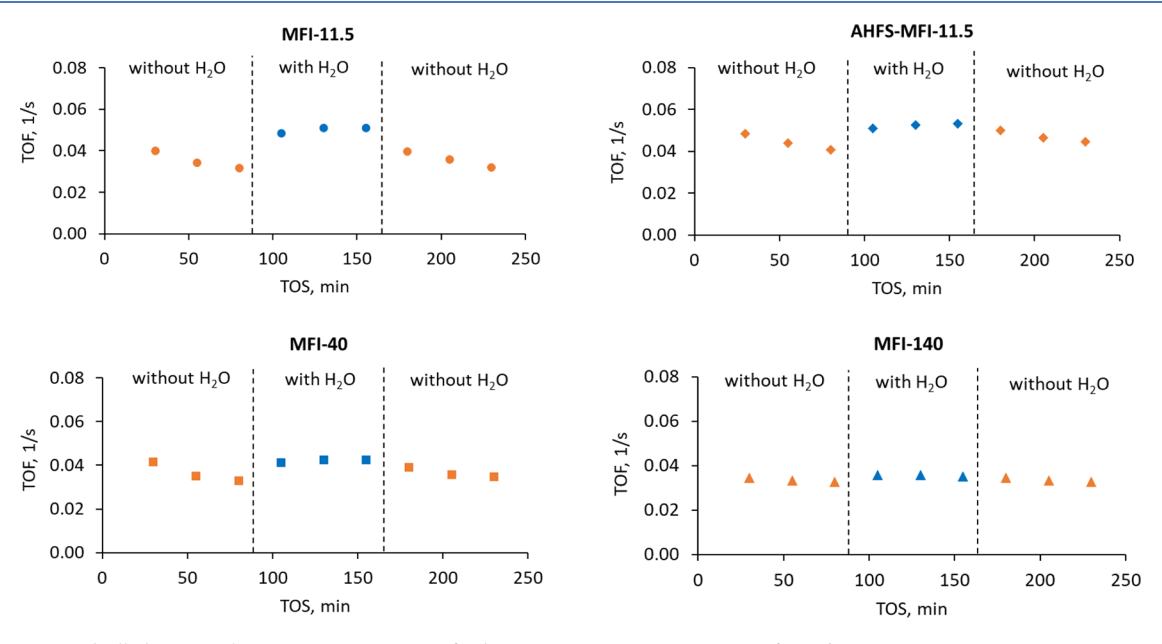


Figure 4. Cumene dealkylation with intermittent water co-feeding at a reaction temperature of 300 $^{\circ}$ C over MFI-11.5, AHFS-MFI-11.5, and MFI-40 and at a reaction temperature of 350 $^{\circ}$ C over MFI-140, $P_{\text{cumene}} = 0.5 \text{ kPa}$, and $P_{\text{water}} = 3.5 \text{ kPa}$.

for the n-hexane cracking reaction. Interestingly, the results show that there is no difference in the rates of cumene conversion on the zeolite before and after pulsed water treatment, as shown in Figure 3. Therefore, this observation implies that the synergistic EFAL-BAS sites are not responsible for the enhanced reaction rate of cumene dealkylation over H-ZSM-5 with high Brønsted acid site densities in the presence of water. The different roles of water in the alkane cracking and cumene dealkylation are likely related to the difference in the mechanism of these reactions. This observation further suggests that the more facile activation of cumene does not benefit from adjacent Lewis cations in the vicinity of framework Brønsted sites to the same extent that more demanding alkane cracking reactions do. We note that the MFI-11.5 catalyst introduces numerous new features and attributes that are not present in the other catalysts studied here. 51,52 The MFI 11.5 sample undergoes a great deal of structural evolution from its parent form upon simple heating under ambient air to reaction conditions. Many new features and non-framework species are created during the simple sample heating. Even the trace levels of moisture found in air can dramatically influence the distribution of Al species, so

while the other catalysts studied here can be considered rather stable under the mild reaction conditions explored here, the same cannot be said for the parent MFI 11.5 sample, which may in part explain the complex and quite different behavior from the other species. Not only does this sample contain extra-framework species that evolve during catalyst pretreatment but is also significantly more sensitive to structural changes in the presence of water than the other catalysts studied here. The co-presence of extra-framework aluminum species, paired sites, and water molecules inside MFI-11.5 pores create a more complicated system than AHFS-MFI-11.5 and MFI-40 catalysts where only framework site density and location are modified. For this chemistry, however, the role of synergistically active sites does not promote cumene deal-kylation chemistry.

3.4. Influence of Water Co-Feed on Cumene Deal-kylation Rates. In this section, the effect of water is investigated based on water co-feeding experiments in cumene dealkylation over different H-ZSM-5 zeolites. It can be seen from Figure 4 that water enhances the turnover frequency of cumene dealkylation over all studied catalysts. However, the effect of water on enhancing cumene dealkylation rates over in

MFI-140 was less pronounced and required a higher reaction temperature than other H-ZSM-5 zeolites (Figures 4 and S9). Interestingly, this enhancement effect of water is reversible, as shown by intermittent water co-feeding experiments. These results suggest that the influence of water on cumene dealkylation is due to the stabilization of reaction intermediates or transition states rather than inducing any irreversible change to the zeolite structure, at least for the samples that do not contain high populations of extra framework Al species.

Irreversible changes to the zeolite by exposure to water vapor under more severe conditions are well-known. Zeolites with low or moderate Si/Al ratios undergo dealumination in the presence of water vapor at a high temperature (≥450 °C),⁵³ which is much higher than the reaction temperature in our study. In addition, the increase of turnover frequency with water co-feeding provides further evidence to suggest that cumene dealkylation over the zeolite samples in this study is not limited by diffusion of reactants to active sites under these reaction conditions.

To decouple the effect of water on reaction kinetics from catalyst deactivation, initial rates in separate reaction runs with and without water co-feeding were determined by extrapolating to zero-minute TOS. Table 3 clearly shows that co-feeding

Table 3. Initial Turnover Frequency (1/s) and Rate Enhancement Percentage of Cumene Dealkylation over Different Zeolites in the Absence and Presence Water at 300 °C.

catalysts	MFI-11.5	AHFS-MFI-11.5	MFI-40
$P_{\text{water}} = 0 \text{ kPa}$	0.055	0.050	0.045
$P_{\text{water}} = 3.5 \text{ kPa}$	0.073	0.063	0.056
rate enhancement, %	32.7	26.0	24.4

water facilitates cumene dealkylation over different zeolites to different extents. Reaction over MFI-11.5 exhibits the most significant enhancement in rate per proton from water cofeeding, followed by AHFS-MFI-11.5 and MFI-40. Kinetic analysis by measuring the reaction order, activation energy, and activation entropy of cumene dealkylation reveals the reason for this enhancement effect of water present inside zeolite pores, as described in the following section.

3.5. Kinetic Role of Brønsted Acid Sites and Water. The partial pressure of cumene was varied to determine the reaction order with respect to cumene in the absence and presence of water (Figure S5). The reaction order of cumene dealkylation over different zeolites is 1st order with respect to cumene at low partial pressures of cumene. The first-order reaction rate with respect to cumene partial pressure on an unsaturated catalyst surface is in agreement with previous proposals that the C-C bond cleavage of adsorbed cumene is the rate-determining step. 7,8 It is evident that cumene molecules undergo significant rates of dealkylation at temperatures below 300 °C, which is much lower than those required to obtain comparable rates for alkane cracking, where protonation is far more demanding. 11,22-24 In addition, reactions over MFI-140 and AHFS-MFI-11.5 shift to the 0th order with respect to cumene at high partial pressures of cumene (Figure 5c-f), indicating that these catalysts can become saturated under these conditions and are not limited by internal mass transfer.

In order to obtain more accurate activation enthalpies and entropies, experiments were performed at lower temperatures where low conversions are readily achieved as discussed earlier (Figure S6, AHFS-MFI-11.5 and MFI-140 with co-fed water showed conversions below 8.0 and 1.5%, respectively). As can be seen in Figure 5, in the presence of both water and cumene in the temperature range from 250 to 260 °C, first-order rate constants are readily achieved at the lowest temperatures studied (Figure 5a,b), with coverages of both water and cumene decreasing at higher temperatures. Because the local cluster size of water may vary with temperatures at a given partial pressure, it was confirmed that the pressures utilized to evaluate the 0th order kinetic regime with respect to cumene in the presence of co-fed water are achieved at both the highest and lowest temperatures used (Figure 5c-f). The achievement of first- and zero-order reactions in the given temperature range, coupled with low conversions, allows the accurate assessment of kinetic rates in the presence of cumene and water co-fed to better understand the intriguing kinetic role of water on stabilization of transition states and kinetically relevant adsorbed intermediates.

Both apparent (1st order) and intrinsic (0th order) activation entropies and enthalpies are shown in Table 4. When compared with the data in the absence of co-fed water, it is revealed that over both catalysts, the apparent and intrinsic activation enthalpies significantly increase over both catalysts when water is incorporated. This is accompanied by a significant reduction in activation entropy. The enhanced rates reported in Figure 4 and Table 3 due to water incorporation are entropically driven. Interestingly, the increased intrinsic activation entropies reported in the presence of water that give rise to enhanced rates in both catalysts still exhibit a slightly negative activation entropy, implying an early transition state in both reaction environments.

The reason for the significant enhancement in activation enthalpy with consequent activation entropy increases under these reaction environments can be ascribed to a variety of potential causes. The presence of water is known to result in delocalized hydronium ion clusters which may give rise to weaker hydronium ions with more degrees of freedom, hence higher intrinsic and apparent activation entropy and enthalpy values. Alternatively, if cumene interactions directly with the zeolite surface were required, the displacement of water molecules would also result in an enthalpy penalty, with potential entropic gains as the hydrogen bonding network in the water cluster is disrupted. Water incorporation tends to not exhibit traditional competitive adsorption behavior. We have recently shown that some polar reactants (ethers) in the presence of strongly binding co-adsorbates that exhibit traditional Langmuir-Hinshelwood competitive adsorption behavior actually exhibit an improved ability to compete for active sites when water is co-fed. 54 This was attributed to the delocalized nature of hydronium ion clusters that are created. Such modifications in rates of acid-catalyzed reactions are quite common with polar reactants where hydrogen bonding is prevalent, but reported enhancements in rates of C-C bond activation in hydrocarbons like cumene are rare. Reactions such as n-alkane cracking do not exhibit similar enhancements in rate due to the presence of water. This could lead one to suggest that the primary discrepancy between the two families of hydrocarbon chemistries (alkane activation and cumene dealkylation) relies not only on the local environment but also on the deprotonation energy required to facilitate the reaction. The greater proton affinity of cumene may enable facile

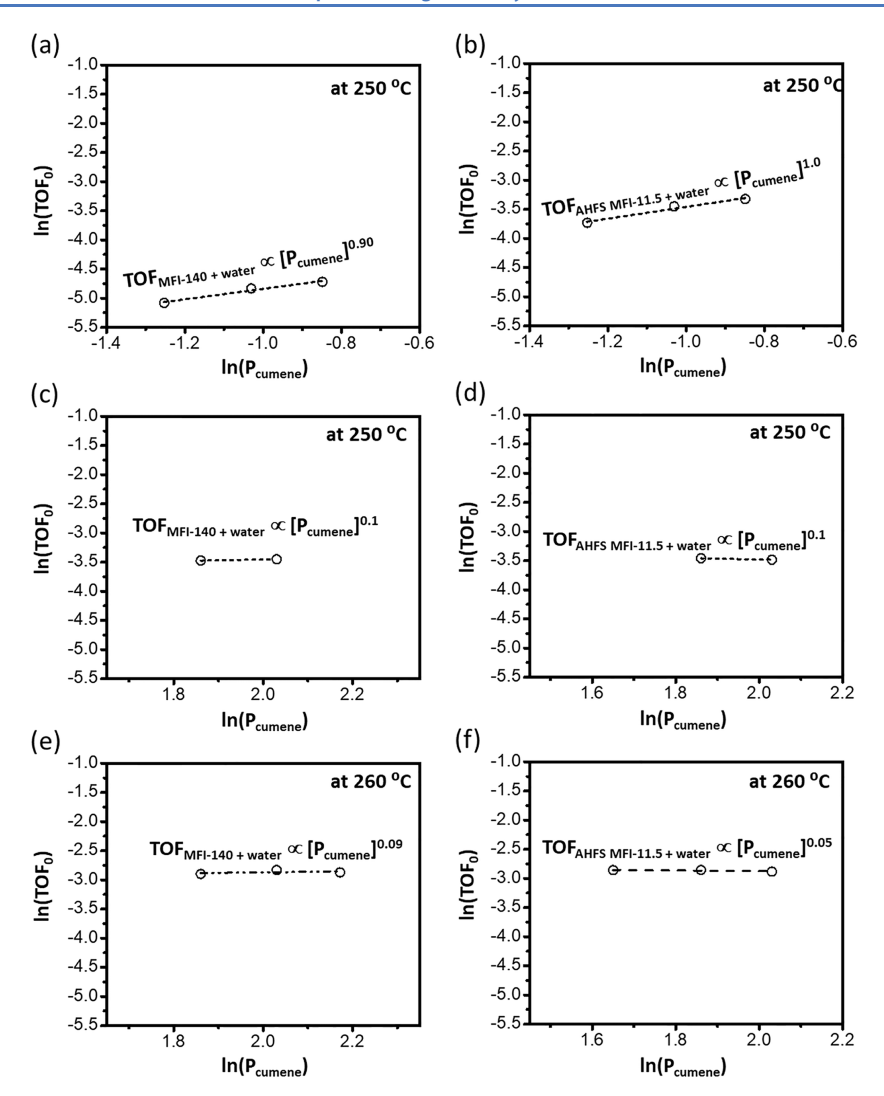


Figure 5. Cumene dealkylation reaction in the 1st and 0th order regimes over (a, c, e) MFI-140 and (b, d, f) AHFS-MFI-11.5 in the presence of water ($P_{\text{water}} = 3.5 \text{ kPa}$) at 250 and 260 °C.

Table 4. Apparent and Intrinsic Activation Energies, Enthalpies, and Entropies Measured in the Temperature Range from 250 to 260 $^{\circ}$ C in the Presence of Water ($P_{\text{water}} = 3.5 \text{ kPa}$)

	catalysts	AHFS-MFI-11.5 + H_2O	$MFI-140 + H_2O$
zero-order regime	intrinsic activation energy E_{int} (kJ/mol) ^a	140.4 ± 4.1	133.1 ± 6.1
	intrinsic activation enthalpy ΔH_{int} (kJ/mol) ^b	136.0 ± 4.1	128.7 ± 6.0
	intrinsic activation entropy $\Delta S_{\text{int}} (J/\text{mol-K})^b$	-18.2 ± 7.8	-32.5 ± 11.4
first-order regime	apparent activation energy E_{app} (kJ/mol) ^a	59.3 ± 1.5	64.6 ± 1.6
	apparent activation enthalpy $\Delta H^{\ddagger}_{ ext{ app }}\left(ext{kJ/mol} ight)^{b}$	54.9 ± 1.5	60.2 ± 1.6
	apparent activation entropy $\Delta S^{\ddagger}_{ ext{app}} \left(extsf{J/mol} \cdot extsf{K} ight)^{b}$	-176 ± 2.9	-174.6 ± 3.0

^aObtained from Arrhenius plot. ^bCalculated from transition state theory. The standard errors are estimated from the least squares method.

protonation and reaction of cumene when compared with less reactive hydrocarbon counterparts. These aspects would greatly benefit from follow-up theoretical studies.

The mechanism of the alkylation of benzene with propylene, which is the reverse reaction of cumene dealkylation, over Brønsted acid sites was proposed to proceed through the C–C bond formation between benzene and surface propoxy species. Weckhuysen and co-workers have applied spectrometry techniques to confirm the presence of surface ethoxy species and carbocationic arenium ion/ σ -complexes (i.e., Wheland-type reaction intermediates) in the ethylation of benzene over zeolites. However, the six-membered ring of

these Wheland- intermediates is stable and may lead to a high energy barrier, which is in contrast to the moderate apparent activation energy of cumene dealkylation over H-ZSM-5 zeolites (Table 2). Therefore, one may speculate a putative transition state for cumene dealkylation over H-ZSM-5 with a backside attack by an oxygen atom at the central isopropyl carbon (Scheme S1). For illustrative purposes, we have included in Scheme S1 a second adjacent proton that could interact with the charged surface intermediate and further modify the activation barrier; however, we note that these effects appear to be less significant than confinement effects, as discussed in Section 3.2.

Interestingly, the effect of water co-feeding is consistent for reactions over MFI-140 and AHFS-MFI-11.5 with the negligible presence of extra-framework aluminum species. It is shown in Table 2 and Table 4 that the presence of water in reactions over these catalysts increases the apparent and intrinsic activation enthalpy, which is compensated by less negative apparent activation entropy. As discussed earlier, it is well known that protons in Brønsted zeolites could become delocalized and form hydronium ion clusters $H_3O^+(H_2O)_n$ in the presence of water molecules inside zeolite pores. 35,36 It is also worth mentioning that water molecules are unlikely to compete for adsorption sites with cumene since the heat of adsorption over H-ZSM-5 zeolites of water is about 51 kJ/ mol, 59 which is lower than the estimated heat of adsorption of cumene measured on the H-ZSM-5 zeolites used here (89-101 kJ/mol). In fact, ab initio molecular dynamics (AIMD) simulations proved the formation of hydronium ion clusters in the presence of water and cyclohexanol, which is a highly competitive adsorbed reactant, in microporous BEA zeolite.⁶ H MAS NMR results (Figures S16 and S17) also appear to indicate that cumene can readily interact with Brønsted acid sites in the presence of water even at low to moderate temperatures. For a reaction such as cumene dealkylation, it is therefore unlikely that water is competitively adsorbing on the surface in a standard Langmuir-Hinshelwood sense and impeding cumene adsorption, rather cumene is most likely able to compete quite well for surface sites and will likely interact with a delocalized hydronium ion water cluster instead.

On the one hand, the enhancement in rate was observed upon water co-feeding for cumene conversion over MFI-140, which has mainly isolated acid sites and is unlikely to benefit from the cooperative effect of site proximity in the presence of water. We speculate that the interaction of cumene with hydronium ion clusters instead of framework protons enables a looser reaction transition state with more degrees of freedom, resulting in a less negative activation entropy. The traditional compensation effect often observed is also observed in these cases (Figure S10). Interestingly, the enhancement upon incorporation of water requires higher temperatures over MFI-140 when compared to the catalysts that contain more proximate sites and acid sites in more confined environments such as AHFS-MFI-11.5 and MFI-40. One may speculate that this result can be explained by the entropically beneficial effect of paired acid sites and acid site location on the promotion of water enhancement in rate; however, we note that we have shown in prior sections that paired sites alone in the absence of water do not appear to entropically enhance reaction rates significantly. This effect should be a function of the size of the delocalized hydronium cluster, which may be probed by altering the water partial pressure to examine the influence of local water concentration inside zeolite pores. Interestingly, after the incorporation of modest water amounts, the enhancement effect of water on cumene dealkylation becomes independent of the partial pressure of water, as shown in Figure S11. It is known that the concentration of hydronium ions inside zeolite pores only depends on the Brønsted acid site density, with entropic benefits of a function of the number of water molecules. The higher the partial pressure of water, the more hydrated the hydronium ion clusters become. In addition, Li et al. found that the proton is only extended to about two water molecules from the original site in MCM-41-SO₃H catalysts, which implies that the positive charge in the hydronium cluster is close to the negative charge on the

catalyst surface.³³ Therefore, while we have shown that proximate sites appear to not be the predominant factor for rate enhancement for cumene dealkylation under dry conditions, the role of Al density and site proximity on water cluster size and rate modifications in the presence of water clusters requires further study. An intriguing aspect that further illustrates this point is the comparison of activation enthalpies measured at low temperatures, as reported in Table 4; in contrast, those at high temperatures, shown in Table 3, reveal that the enthalpic changes upon water incorporation are much more pronounced when measured at lower temperatures than at high temperatures, while the water partial pressure is the same in both scenarios. At lower temperatures, while the general trends are the same, the first-order activation enthalpies are more elevated, as are the activation entropies. This reflects a larger water cluster size that gives rise to this shift in behavior.

Table S4 shows a decrease in apparent activation enthalpy and more negative apparent activation entropy in the presence of water for reactions over MFI-11.5 that has not been washed by AHFS to remove extra lattice species. This different behavior compared to AHFS-MFI-11.5 and MFI-40 is likely due to the presence of extra-framework aluminum species in MFI-11.5 and further revealed by the volcano curve where the initial TOF of cumene dealkylation was plotted with varying partial pressure of water (Figure S11). We note here that this catalyst is quite sensitive to moisture at high temperatures, and while positive consequences of water on reaction rates may result, increased pressures may also damage the zeolite structure. Furthermore, given the fact that this zeolite contains both the highest density of sites and extra framework species, the high partial pressure of water may lead to the formation of large clusters of hydrated extra-framework aluminum species, which act as spatial constraints inside MFI pores and hence create a more confined environment within the pores of the catalyst, which would result in the reduced activation enthalpies as consistent with the discussion above. The enhancement also appears to be reversible, implying that the hydrated form of these extra lattice alumina clusters modifies transition states to a greater degree than dehydrated Lewis

It is acknowledged that the fraction of extra-framework aluminum species in H-ZSM-5 zeolites with low Si/Al ratios like MFI-11.5 is considerable. However, the similar initial turnover frequency between MFI-11.5 and AHFS-MFI-11.5 (Figure S11) implies that extra-framework species do not play the most critical role on the cumene dealkylation rates under these mild reaction conditions, but the presence of these extraframework species may influence the catalyst deactivation, and we also note that extra lattice species are mobile in the presence of water, with varying location as well as aggregate size as a function of pretreatment and reaction conditions. Therefore, it is suggested that the cumene dealkylation rate is primarily influenced by the environment surrounding the Brønsted acid sites (proximity and/or location). In addition, it is recognized that MFI zeolites may be subject to internal diffusion limitations that corrupt observed reaction rates, particularly at low Si/Al ratios. 46 However, in this study, the higher reaction rates normalized per Brønsted acid site, higher apparent activation energy over MFI-11.5 when compared to MFI zeolites with a lower acid site density (Figure 1, Tables 1 and S4), and the reversible enhancement effect of the intermittent co-feeding of water on the rate of cumene

dealkylation over MFI zeolites (Figure 4) imply that reactions over these catalysts are unlikely to be limited by internal diffusion.

3.6. Catalyst Deactivation in Cumene Dealkylation: Effect of Extra-Framework Aluminum Species, Reaction Temperature, and the Presence of Water. The products of cumene dealkylation are propylene and benzene, with an expected molar ratio of 1:1. However, propylene is a reactive olefin that can readily undergo subsequent reactions such as oligomerization over H-ZSM-5 zeolites and form coke even at low temperatures. The selectivity toward propylene is slightly lower than that toward benzene for reactions over different zeolites (Figure S5a). This observation suggests that propylene may continue to oligomerize and form heavier compounds in zeolites which is the main cause of catalyst deactivation over time on stream.

Catalyst deactivation during cumene dealkylation was evaluated by plotting the turnover number—turnover frequency correlation, as previously described. The influence of Brønsted acid site density and the role of extra-framework aluminum species on catalyst stability in cumene dealkylation were evaluated, as shown in Figure 6.

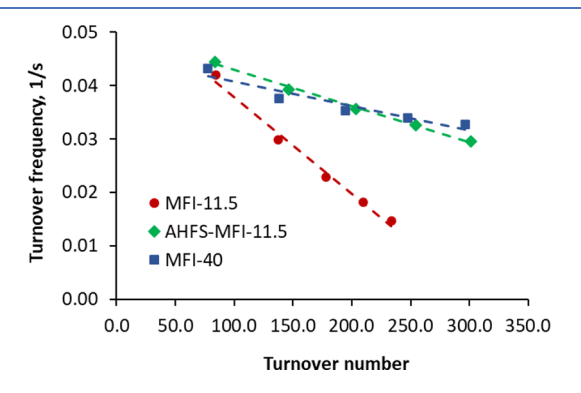


Figure 6. Deactivation plots of different zeolites in cumene dealkylation at a reaction temperature of 300 $^{\circ}$ C, P_{cumene} = 0.5 kPa.

Catalyst deactivation tends to increase with Brønsted acid site density by comparing TON-TOF plots of MFI-40 and AHFS-MFI-11.5. In fact, propylene oligomerization is a sequential reaction that should enhance with the increasing Brønsted acid site density or the presence of adjacent Brønsted acid sites. This result is in agreement with the previous literature that found that the turnover frequency of propylene oligomerization rates over close Brønsted acid sites could be up to one order of magnitude higher than that over isolated Brønsted acid sites, which has been attributed to the transition state entropy gain over proximate sites. ^{13,62}

In addition, it seems that the presence of extra-framework aluminum species in MFI-11.5 leads to a faster catalyst deactivation compared to AHFS-MFI-11.5, which has a similar Brønsted acid site density but with an insignificant amount of extra-framework aluminum species. It has been reported that these extra-framework aluminum species increase the adsorption enthalpy of adsorbed molecules. Consequently, coke precursors generated from propylene oligomerization may adsorb more strongly to the acid sites and further undergo coke formation. Additional extra-lattice species may also impede the diffusion paths of exiting products. In fact, it was reported by many research groups that the presence of extra-framework aluminum species in zeolites correlates with

increased catalyst deactivation rates in various reactions such as n-heptane cracking, toluene disproportionation, toluene alkylation with ethylene, n-butene isomerization, and cumene—toluene transalkylation. $^{64-67}$

The presence of water not only facilitates cumene dealkylation by increasing transition state entropy but also reduces catalyst deactivation over reaction time on stream, as shown in Figures 7 and S12–S14. This effect of water on

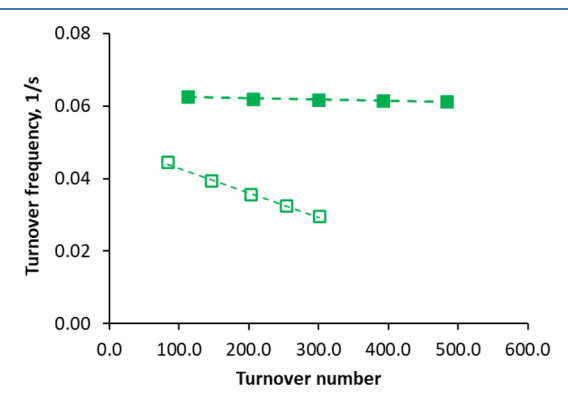


Figure 7. Effect of water co-feeding on deactivation of AHFS-MFI-11.5 at a reaction temperature of 300 °C, $P_{\rm cumene} = 0.5$ kPa, $P_{\rm water} = 0$ kPa (□); $P_{\rm cumene} = 0.5$ kPa, $P_{\rm water} = 3.5$ kPa (■).

catalyst stability is consistent for catalysts with different Brønsted acid site densities and with the presence or absence of extra-framework aluminum species.

It is acknowledged that Brønsted acid sites are delocalized to form hydronium ion clusters inside zeolite pores that can still catalyze reactions such as alcohol dehydration. 38,39 Therefore, these hydronium ion clusters should be able to catalyze a facile reaction such as propylene oligomerization. On the other hand, the heat of water adsorption on H-ZSM-5 zeolites is about 51 kJ/mol measured experimentally,⁵⁹ while propylene adsorption on H-ZSM-5 forms a stable carbenium ion.⁶⁸ Another light olefin, such as ethylene, has a heat of adsorption of 46 kJ/mol on H-ZSM-5 zeolite based on hybrid MP2:DFT calculation.⁶⁹ Therefore, water is less likely to enhance catalyst stability by competing for adsorption sites with propylene molecules and inhibiting propylene oligomerization. In fact, the selectivity toward propylene is almost unchanged in the absence and presence of water for AHFS-MFI-11.5 and MFI-40 zeolites (Figure S9a). This observation implies that water does not stop propylene from further reactions by competitive adsorption.

It has been discussed that water molecules inside zeolite pores tend to delocalize the proton and improve Brønsted acid site proximity. On the other hand, Bell and co-workers found that the presence of oligomers on the adjacent Brønsted acid site increases activation energy for propylene trimerization, whereas the acid site proximity does not affect propylene dimerization, resulting in a higher selectivity to dimers. 12 As a result, the accumulation of heavy compounds and coke from propylene oligomerization is reduced, which leads to a more stable catalyst. Therefore, the enhancement of catalyst stability in the presence of water can be attributed to the effect of water molecules on facilitating Brønsted acid site proximity. However, we note in this case that propylene dimers are not observed in significant quantities as one might expect if this were the case. Alternatively, we hypothesize that water may promote a more stable intermediate where the frameworkACS Catalysis pubs.acs.org/acscatalysis Research Article

bound proton is shared between a water molecule and the olefin, lowering the energy of the intermediate but leading to a higher intrinsic activation energy for coupling. This stabilization effect of water has been shown in alcohol dehydration, where water enthalpically stabilizes adsorbed intermediate to a greater extent than the relevant transition state, leading to a higher energy barrier for propene formation. The root cause of enhancing catalyst stability during cumene deal-kylation in the presence of water requires further study.

4. CONCLUSIONS

Cumene dealkylation rates are significantly enhanced as the density of Brønsted acid sites increases. Interestingly, the reaction rate also increases in the presence of water molecules with a reversible effect. Based on detailed reaction kinetics, it is evident that the presence of acid sites in more confined environments promotes enhanced activity by enthalpically stabilizing kinetically relevant intermediates and transition states, while the presence of water conversely improves the turnover frequency in reactions over H-ZSM-5 zeolites by increasing the entropy of the transition state. We propose that the formation of hydrated hydronium ions in the presence of water may create a looser transition state with more degrees of freedom. It is also worth mentioning that the EFAL-BAS synergistic sites generated by pulsing water over H-ZSM-5 with a low Si/Al ratio do not appear to significantly influence cumene dealkylation rates under the reaction conditions studied. However, the presence of extra-framework species in H-ZSM-5 zeolites may increase coking. Catalyst stability during cumene dealkylation can be improved by adding moisture, removing extra-framework aluminum species, and optimizing reaction temperature. These findings are of great practical importance to modifying rates of complex reactions involving cleavage of aromatic alkane functional groups, including decomposition of polystyrene and understanding benzene formation in catalytic cracking.

ASSOCIATED CONTENT

Supporting Information

The Supporting Information is available free of charge at https://pubs.acs.org/doi/10.1021/acscatal.2c05759.

Catalyst characterization of different H-ZSM-5 zeolites; linear regression fitting of cumene dealkylation rate versus fraction of aluminum in pairs; effect of intermittent co-feeding water on cumene dealkylation over MFI-140 at 300 °C; derivation of cumene dealkylation rate by transition state theory; effect of water partial pressure on cumene dealkylation over H-ZSM-5 zeolites; catalyst deactivation during cumene dealkylation; in-situ NMR spectra of cumene conversion over zeolites in the presence and absence of water; and SEM images of H-ZSM-5 zeolites (PDF)

AUTHOR INFORMATION

Corresponding Author

Steven P. Crossley — School of Chemical, Biological and Materials Engineering, University of Oklahoma, Norman, Oklahoma 73019, United States; orcid.org/0000-0002-1017-9839; Phone: +1 (405) 325-5930;

Email: stevencrossley@ou.edu; Fax: +1 (405) 325-5813

Authors

Han K. Chau — School of Chemical, Biological and Materials Engineering, University of Oklahoma, Norman, Oklahoma 73019, United States; orcid.org/0000-0003-3172-0257

Hien D. Mai — School of Chemical, Biological and Materials Engineering, University of Oklahoma, Norman, Oklahoma 73019, United States

Abhishek Gumidyala — School of Chemical, Biological and Materials Engineering, University of Oklahoma, Norman, Oklahoma 73019, United States

Tram N. Pham — School of Chemical, Biological and Materials Engineering, University of Oklahoma, Norman, Oklahoma 73019, United States

Dai-Phat Bui — School of Chemical, Biological and Materials Engineering, University of Oklahoma, Norman, Oklahoma 73019, United States; orcid.org/0000-0002-3886-9022

Andrew D. D'Amico – School of Chemical, Biological and Materials Engineering, University of Oklahoma, Norman, Oklahoma 73019, United States

Ismaeel Alalq — School of Chemical, Biological and Materials Engineering, University of Oklahoma, Norman, Oklahoma 73019, United States

Daniel T. Glatzhofer – Department of Chemistry and Biochemistry, University of Oklahoma, Norman, Oklahoma 73019, United States

Jeffery L. White — School of Chemical Engineering, Oklahoma State University, Stillwater, Oklahoma 74078, United States; orcid.org/0000-0003-4065-321X

Complete contact information is available at: https://pubs.acs.org/10.1021/acscatal.2c05759

Author Contributions

H.C. and H.M. contributed equally to this work.

Notes

The authors declare no competing financial interest.

ACKNOWLEDGMENTS

The authors are grateful for the support from National Science Foundation under the Grant No. CHE-2154399, CHE-2154398, and EFMA-2029394 to carry out this research. We thank Dr. Daniel E. Resasco for helpful technical discussions and Huy P. Nguyen for his assistance with product analysis.

REFERENCES

- (1) Zhao, Y.; Wojciechowski, B. The consequences of steam dilution in catalytic cracking: I. Effect of steam dilution on reaction rates and activation energy in 2-methylpentane cracking over USHY. *J. Catal.* **1996**, *163*, 365–373.
- (2) Di Iorio, J. R.; Nimlos, C. T.; Gounder, R. Introducing Catalytic Diversity into Single-Site Chabazite Zeolites of Fixed Composition via Synthetic Control of Active Site Proximity. ACS Catal. 2017, 7, 6663–6674.
- (3) Margarit, V. J.; Osman, M.; Al-Khattaf, S.; Martinez, C.; Boronat, M.; Corma, A. Control of the reaction mechanism of alkylaromatics transalkylation by means of molecular confinement effects associated to zeolite channel architecture. *ACS Catal.* **2019**, *9*, 5935–5946.
- (4) Al-Khattaf, S.; Ali, S. A.; Aitani, A. M.; Žilková, N.; Kubička, D.; Čejka, J. Recent advances in reactions of alkylbenzenes over novel zeolites: the effects of zeolite structure and morphology. *Catal. Rev.* **2014**, *56*, 333–402.
- (5) Serra, J. M.; Guillon, E.; Corma, A. A rational design of alkylaromatics dealkylation—transalkylation catalysts using C8 and C9 alkyl-aromatics as reactants. *J. Catal.* **2004**, 227, 459—469.

- (6) Al-Khattaf, S.; De Lasa, H. The role of diffusion in alkylbenzenes catalytic cracking. *Appl. Catal., A* **2002**, 226, 139–153.
- (7) Corma, A.; Wojciechowski, B. The catalytic cracking of cumene. *Catal. Rev.: Sci. Eng.* **1982**, *24*, 1–65.
- (8) Corma, A.; Fierro, J.; Montan, R.; Tomas, F. On the mechanism of cumene dealkylation: the interaction of cumene molecules on silica-alumina surfaces. *J. Mol. Catal.* **1985**, *30*, 361–372.
- (9) Corma, A. State of the art and future challenges of zeolites as catalysts. *J. Catal.* **2003**, *216*, 298–312.
- (10) Dědeček, J.; Tabor, E.; Sklenak, S. Tuning the aluminum distribution in zeolites to increase their performance in acid-catalyzed reactions. *ChemSusChem* **2019**, *12*, 556–576.
- (11) Song, C.; Chu, Y.; Wang, M.; Shi, H.; Zhao, L.; Guo, X.; Yang, W.; Shen, J.; Xue, N.; Peng, L.; et al. Cooperativity of adjacent Brønsted acid sites in MFI zeolite channel leads to enhanced polarization and cracking of alkanes. *J. Catal.* **2017**, 349, 163–174.
- (12) Mlinar, A. N.; Zimmerman, P. M.; Celik, F. E.; Head-Gordon, M.; Bell, A. T. Effects of Brønsted-acid site proximity on the oligomerization of propene in H-MFI. *J. Catal.* **2012**, 288, 65–73.
- (13) Tabor, E.; Bernauer, M.; Wichterlová, B.; Dedecek, J. Enhancement of propene oligomerization and aromatization by proximate protons in zeolites; FTIR study of the reaction pathway in ZSM-5. *Catal. Sci. Technol.* **2019**, *9*, 4262–4275.
- (14) Kester, P. M.; Crum, J. T.; Li, S.; Schneider, W. F.; Gounder, R. Effects of Brønsted Acid Site Proximity in Chabazite Zeolites on OH Infrared Spectra and Protolytic Propane Cracking Kinetics. *J. Catal.* **2021**, 395, 210–226.
- (15) Li, G.; Wang, B.; Chen, B.; Resasco, D. E. Role of water in cyclopentanone self-condensation reaction catalyzed by MCM-41 functionalized with sulfonic acid groups. *J. Catal.* **2019**, 377, 245–254.
- (16) Gołąbek, K.; Tabor, E.; Pashkova, V.; Dedecek, J.; Tarach, K.; Góra-Marek, K. The proximity of aluminium atoms influences the reaction pathway of ethanol transformation over zeolite ZSM-5. *Commun. Chem.* **2020**, *3*, 25.
- (17) Jones, A. J.; Carr, R. T.; Zones, S. I.; Iglesia, E. Acid strength and solvation in catalysis by MFI zeolites and effects of the identity, concentration and location of framework heteroatoms. *J. Catal.* **2014**, 312, 58–68.
- (18) Jones, A. J.; Iglesia, E. The strength of Brønsted acid sites in microporous aluminosilicates. ACS Catal. 2015, 5, 5741–5755.
- (19) Gounder, R.; Iglesia, E. The catalytic diversity of zeolites: confinement and solvation effects within voids of molecular dimensions. *Chem. Commun.* **2013**, *49*, 3491–3509.
- (20) Jones, A. J.; Zones, S. I.; Iglesia, E. Implications of transition state confinement within small voids for acid catalysis. *J. Phys. Chem.* C **2014**, *118*, 17787–17800.
- (21) Gounder, R.; Iglesia, E. Effects of partial confinement on the specificity of monomolecular alkane reactions for acid sites in side pockets of mordenite. *Angew. Chem., Int. Ed.* **2010**, *49*, 808–811.
- (22) Schallmoser, S.; Ikuno, T.; Wagenhofer, M.; Kolvenbach, R.; Haller, G.; Sanchez-Sanchez, M.; Lercher, J. Impact of the local environment of Brønsted acid sites in ZSM-5 on the catalytic activity in n-pentane cracking. *J. Catal.* **2014**, *316*, 93–102.
- (23) Zhang, Y.; Zhao, R.; Sanchez-Sanchez, M.; Haller, G. L.; Hu, J.; Bermejo-Deval, R.; Liu, Y.; Lercher, J. A. Promotion of protolytic pentane conversion on H-MFI zeolite by proximity of extra-framework aluminum oxide and Brønsted acid sites. *J. Catal.* **2019**, 370, 424–433.
- (24) Chen, K.; Abdolrahmani, M.; Horstmeier, S.; Pham, T. N.; Nguyen, V. T.; Zeets, M.; Wang, B.; Crossley, S.; White, J. L. Brønsted—Brønsted Synergies between Framework and Noncrystalline Protons in Zeolite H-ZSM-5. ACS Catal. 2019, 9, 6124—6136.
- (25) Pham, T. N.; Nguyen, V.; Wang, B.; White, J. L.; Crossley, S. Quantifying the Influence of Water on the Mobility of Aluminum Species and Their Effects on Alkane Cracking in Zeolites. *ACS Catal.* **2021**, *11*, 6982–6994.
- (26) Fritz, P. O.; Lunsford, J. H. The effect of sodium poisoning on dealuminated Y-type zeolites. *J. Catal.* **1989**, *118*, 85–98.

- (27) Li, G.; Wang, B.; Resasco, D. E. Water-mediated heterogeneously catalyzed reactions. ACS Catal. 2019, 10, 1294–1309.
- (28) Heard, C. J.; Grajciar, L.; Uhlík, F.; Shamzhy, M.; Opanasenko, M.; Čejka, J.; Nachtigall, P. Zeolite (In) Stability under Aqueous or Steaming Conditions. *Adv. Mater.* **2020**, *32*, No. 2003264.
- (29) Zhang, L.; Chen, K.; Chen, B.; White, J. L.; Resasco, D. E. Factors that determine zeolite stability in hot liquid water. *J. Am. Chem. Soc.* **2015**, *137*, 11810–11819.
- (30) Zhao, Z.; Bababrik, R.; Xue, W.; Li, Y.; Briggs, N. M.; Nguyen, D.-T.; Nguyen, U.; Crossley, S. P.; Wang, S.; Wang, B.; et al. Solvent-mediated charge separation drives alternative hydrogenation path of furanics in liquid water. *Nat. Catal.* **2019**, *2*, 431–436.
- (31) Xue, N.; Vjunov, A.; Schallmoser, S.; Fulton, J. L.; Sanchez-Sanchez, M.; Hu, J. Z.; Mei, D.; Lercher, J. A. Hydrolysis of zeolite framework aluminum and its impact on acid catalyzed alkane reactions. *J. Catal.* **2018**, 365, 359–366.
- (32) Chen, K.; Damron, J.; Pearson, C.; Resasco, D.; Zhang, L.; White, J. L. Zeolite Catalysis: Water Can Dramatically Increase or Suppress Alkane C–H Bond Activation. *ACS Catal.* **2014**, *4*, 3039–3044.
- (33) Li, G.; Wang, B.; Kobayashi, T.; Pruski, M.; Resasco, D. E. Optimizing the surface distribution of acid sites for cooperative catalysis in condensation reactions promoted by water. *Chem. Catal.* **2021**, *1*, 1065–1087.
- (34) Chen, K.; Kelsey, J.; White, J. L.; Zhang, L.; Resasco, D. Water interactions in zeolite catalysts and their hydrophobically modified analogues. *ACS Catal.* **2015**, *5*, 7480–7487.
- (35) Vjunov, A.; Wang, M.; Govind, N.; Huthwelker, T.; Shi, H.; Mei, D.; Fulton, J. L.; Lercher, J. A. Tracking the Chemical Transformations at the Brønsted Acid Site upon Water-Induced Deprotonation in a Zeolite Pore. *Chem. Mater.* **2017**, *29*, 9030–9042.
- (36) Zeets, M.; Resasco, D. E.; Wang, B. Enhanced chemical activity and wettability at adjacent Brønsted acid sites in HZSM-5. *Catal. Today* **2018**, *312*, 44–50.
- (37) Wang, M.; Jaegers, N. R.; Lee, M.-S.; Wan, C.; Hu, J. Z.; Shi, H.; Mei, D.; Burton, S. D.; Camaioni, D. M.; Gutiérrez, O. Y.; et al. Genesis and Stability of Hydronium Ions in Zeolite Channels. *J. Am. Chem. Soc.* **2019**, *141*, 3444–3455.
- (38) Liu, Y.; Vjunov, A.; Shi, H.; Eckstein, S.; Camaioni, D. M.; Mei, D.; Baráth, E.; Lercher, J. A. Enhancing the catalytic activity of hydronium ions through constrained environments. *Nat. Commun.* **2017**, *8*, 14113.
- (39) Shi, H.; Eckstein, S.; Vjunov, A.; Camaioni, D. M.; Lercher, J. A. Tailoring nanoscopic confines to maximize catalytic activity of hydronium ions. *Nat. Commun.* **2017**, *8*, 15442.
- (40) Eckstein, S.; Hintermeier, P. H.; Olarte, M. V.; Liu, Y.; Baráth, E.; Lercher, J. A. Elementary steps and reaction pathways in the aqueous phase alkylation of phenol with ethanol. *J. Catal.* **2017**, 352, 329–336.
- (41) Liu, Y.; Baráth, E.; Shi, H.; Hu, J.; Camaioni, D. M.; Lercher, J. A. Solvent-determined mechanistic pathways in zeolite-H-BEA-catalysed phenol alkylation. *Nat. Catal.* **2018**, *1*, 141–147.
- (42) Pfriem, N.; Hintermeier, P. H.; Eckstein, S.; Kim, S.; Liu, Q.; Shi, H.; Milakovic, L.; Liu, Y.; Haller, G. L.; Baráth, E.; et al. Role of the ionic environment in enhancing the activity of reacting molecules in zeolite pores. *Science* **2021**, *372*, 952–957.
- (43) Wang, H.; Hou, Y.; Sun, W.; Hu, Q.; Xiong, H.; Wang, T.; Yan, B.; Qian, W. Insight into the Effects of Water on the Ethene to Aromatics Reaction with HZSM-5. ACS Catal. 2020, 10, 5288–5298.
- (44) De Wispelaere, K.; Wondergem, C. S.; Ensing, B.; Hemelsoet, K.; Meijer, E. J.; Weckhuysen, B. M.; Van Speybroeck, V.; Ruiz-Martínez, J. Insight into the Effect of Water on the Methanol-to-Olefins Conversion in H-SAPO-34 from Molecular Simulations and in Situ Microspectroscopy. ACS Catal. 2016, 6, 1991–2002.
- (45) Bollini, P.; Chen, T. T.; Neurock, M.; Bhan, A. Mechanistic role of water in HSSZ-13 catalyzed methanol-to-olefins conversion. *Catal. Sci. Technol.* **2019**, *9*, 4374–4383.

- (46) Chau, H. K.; Resasco, D. E.; Do, P.; Crossley, S. P. Acylation of m-cresol with acetic acid supported by in-situ ester formation on H-ZSM-5 zeolites. J. Catal. 2022, 406, 48-55.
- (47) Dědeček, J.; Kaucký, D.; Wichterlová, B.; Gonsiorová, O. Co²⁺ ions as probes of Al distribution in the framework of zeolites. ZSM-5 study. Phys. Chem. Chem. Phys. 2002, 4, 5406-5413.
- (48) Janda, A.; Bell, A. T. Effects of Si/Al ratio on the distribution of framework Al and on the rates of alkane monomolecular cracking and dehydrogenation in H-MFI. J. Am. Chem. Soc. 2013, 135, 19193-19207.
- (49) Nimlos, C. T.; Hoffman, A. J.; Hur, Y. G.; Lee, B. J.; Di Iorio, J. R.; Hibbitts, D. D.; Gounder, R. Experimental and Theoretical Assessments of Aluminum Proximity in MFI Zeolites and Its Alteration by Organic and Inorganic Structure-Directing Agents. Chem. Mater. 2020, 32, 9277-9298.
- (50) Noh, G.; Shi, Z.; Zones, S. I.; Iglesia, E. Isomerization and β scission reactions of alkanes on bifunctional metal-acid catalysts: Consequences of confinement and diffusional constraints on reactivity and selectivity. J. Catal. 2018, 368, 389-410.
- (51) Chen, K.; Gan, Z.; Horstmeier, S.; White, J. L. Distribution of aluminum species in zeolite catalysts: 27Al NMR of framework, partially-coordinated framework, and non-framework moieties. J. Am. Chem. Soc. 2021, 143, 6669-6680.
- (52) Chen, K.; Horstmeier, S.; Nguyen, V. T.; Wang, B.; Crossley, S. P.; Pham, T.; Gan, Z.; Hung, I.; White, J. L. Structure and Catalytic Characterization of a Second Framework Al (IV) Site in Zeolite Catalysts Revealed by NMR at 35.2 T. J. Am. Chem. Soc. 2020, 142, 7514-7523.
- (53) Ong, L. H.; Dömök, M.; Olindo, R.; van Veen, A. C.; Lercher, J. A. Dealumination of HZSM-5 via steam-treatment. Microporous Mesoporous Mater. 2012, 164, 9-20.
- (54) Chau, H. K.; Nguyen, Q. P.; Jerdy, A. C.; Bui, D.-P.; Lobban, L. L.; Wang, B.; Crossley, S. P. Role of Water on Zeolite-Catalyzed Dehydration of Polyalcohols and EVOH Polymer. ACS Catal. 2023, 13, 1503-1512.
- (55) Rozanska, X.; Barbosa, L.; van Santen, R. A periodic density functional theory study of cumene formation catalyzed by Hmordenite. J. Phys. Chem. B 2005, 109, 2203-2211.
- (56) Jansang, B.; Nanok, T.; Limtrakul, J. Structures and reaction mechanisms of cumene formation via benzene alkylation with propylene in a newly synthesized ITQ-24 zeolite: an embedded ONIOM study. J. Phys. Chem. B 2006, 110, 12626-12631.
- (57) Lei, Z.; Liu, L.; Dai, C. Insight into the reaction mechanism and charge transfer analysis for the alkylation of benzene with propylene over H-beta zeolite. Mol. Catal. 2018, 454, 1-11.
- (58) Chowdhury, A. D.; Houben, K.; Whiting, G. T.; Chung, S.-H.; Baldus, M.; Weckhuysen, B. M. Electrophilic aromatic substitution over zeolites generates Wheland-type reaction intermediates. Nat. Catal. 2018, 1, 23-31.
- (59) Ison, A.; Gorte, R. J. The adsorption of methanol and water on H-ZSM-5. J. Catal. 1984, 89, 150-158.
- (60) Mei, D.; Lercher, J. A. Effects of Local Water Concentrations on Cyclohexanol Dehydration in H-BEA Zeolites. J. Phys. Chem. C 2019, 123, 25255-25266.
- (61) Kofke, T. G.; Gorte, R. A temperature-programmed desorption study of olefin oligomerization in H-ZSM-5. J. Catal. 1989, 115, 233-243.
- (62) Bernauer, M.; Tabor, E.; Pashkova, V.; Kaucký, D.; Sobalík, Z.; Wichterlová, B.; Dedecek, J. Proton proximity-New key parameter controlling adsorption, desorption and activity in propene oligomerization over H-ZSM-5 zeolites. J. Catal. 2016, 344, 157-172.
- (63) van Bokhoven, J. A.; Tromp, M.; Koningsberger, D.; Miller, J.; Pieterse, J.; Lercher, J.; Williams, B.; Kung, H. H. An explanation for the enhanced activity for light alkane conversion in mildly steam dealuminated mordenite: The dominant role of adsorption. J. Catal. 2001, 202, 129-140.
- (64) Wang, Q.; Giannetto, G.; Guisnet, M. Dealumination of zeolites III. Effect of extra-framework aluminum species on the

- activity, selectivity, and stability of Y zeolites in n-heptane cracking. J. Catal. 1991, 130, 471-482.
- (65) Čejka, J.; Vondrová, A.; Wichterlová, B.; Jerschkewitz, H. G.; Lischke, G.; Schreier, E. The effect of extra-framework aluminum in dealuminated ZSM-5 zeolites on the transformation of aromatic hydrocarbons. Collect. Czech. Chem. Commun. 1995, 60, 412-420.
- (66) Wichterlová, B.; Žilkova, N.; Uvarova, E.; Čejka, J.; Sarv, P.; Paganini, C.; Lercher, J. A. Effect of Brønsted and Lewis sites in ferrierites on skeletal isomerization of n-butenes. Appl. Catal., A 1999, 182, 297-308.
- (67) Mavrodinova, V.; Popova, M.; Mihályi, R.; Páł-Borbély, G.; Minchey, C. Transalkylation of toluene with cumene over zeolites Y dealuminated in solid-state: Part II. Effect of the introduced Lewis acid sites. Appl. Catal., A 2003, 248, 197-209.
- (68) Grady, M.; Gorte, R. J. Adsorption of 2-propanol and propene on H-ZSM-5: evidence for stable carbenium ion formation. J. Phys. Chem. 1985, 89, 1305-1308.
- (69) Hansen, N.; Kerber, T.; Sauer, J.; Bell, A. T.; Keil, F. J. Quantum chemical modeling of benzene ethylation over H-ZSM-5 approaching chemical accuracy: a hybrid MP2: DFT study. J. Am. Chem. Soc. 2010, 132, 11525-11538.
- (70) Zhi, Y.; Shi, H.; Mu, L.; Liu, Y.; Mei, D.; Camaioni, D. M.; Lercher, J. A. Dehydration Pathways of 1-Propanol on HZSM-5 in the Presence and Absence of Water. J. Am. Chem. Soc. 2015, 137, 15781-15794.
- (71) Macht, J.; Janik, M. J.; Neurock, M.; Iglesia, E. Mechanistic consequences of composition in acid catalysis by polyoxometalate Keggin clusters. J. Am. Chem. Soc. 2008, 130, 10369-10379.

□ Recommended by ACS

Solvent Mediated Interactions on Alkene Epoxidations in Ti-MFI: Effects of Solvent Identity and Silanol Density

Chris Torres, David W. Flaherty, et al.

JUNE 21, 2023 ACS CATALYSIS

READ 2

Effect of Silver Cations on Propene Aromatization on H-ZSM-5 Zeolite Investigated by ¹³C MAS NMR and FTIR Spectroscopy

Zoya N. Lashchinskaya, Alexander G. Stepanov, et al.

JULY 21, 2023

ACS CATALYSIS

READ

Structure, Location, and Spatial Proximities of Hydroxyls on γ-Alumina Crystallites by High-Resolution Solid-State NMR and DFT Modeling: Why Edges Hold the Key

Ana T. F. Batista, Pascal Raybaud, et al.

APRIL 28, 2023 ACS CATALYSIS

READ C

Surface Diffusion Barriers and Catalytic Activity Driven by **Terminal Groups at Zeolite Catalysts**

Mingbin Gao, Zhongmin Liu, et al.

AUGUST 18, 2023

ACS CATALYSIS

RFAD 🗹

Get More Suggestions >